Biomaterials xxx (xxxx) xxxx

Contents lists available at ScienceDirect

Biomaterials

journal homepage: www.elsevier.com/locate/biomaterials

Retinoic acid-loaded NFL-lipid nanocapsules promote oligodendrogenesis in focal white matter lesion

Dario Carradori[a,b], Yasmine Labrak[a], Véronique E. Miron[c], Patrick Saulnier[b], Joël Eyer[b], Véronique Préat[a], Anne des Rieux[a,*]

[a] Université catholique de Louvain, Louvain Drug Research Institute, Advanced Drug Delivery and Biomaterials, Avenue E. Mounier 73, 1200, Brussels, Belgium
[b] Université d'Angers, Unité de Micro et Nanomédecines Translationnelles, Inserm 1066, CNRS 6021, Institut de Biologie en Santé PBH-IRIS, 49033, Angers, France
[c] MRC Center for Reproductive Health, The Queen's Medical Research Institute, The University of Edinburgh, Edinburgh, United Kingdom

HIGHLIGHTS

- NFL-lipid nanocapsules (NFL-LNC) efficiently encapsulate retinoic acid (RA).
- Primary neural stem cells differentiate towards the oligodendrocyte lineage after incubation with RA-NFL-LNC.
- RA-NFL-LNC promote oligodendrocyte repopulation in focal white matter lesioned rats.
- RA-NFL-LNC is a promising therapeutic system for the treatment of demyelinating diseases.

ARTICLE INFO

Keywords:
Demyelinating diseases
Lipid nanocapsules
Oligodendrogenesis
Neural stem cells
Retinoic acid
Brain

ABSTRACT

Neural stem cells (NSC) are located in restricted areas of the central nervous system where they self-renew or differentiate into neurons, astrocytes or oligodendrocytes. The stimulation of endogenous NSC differentiation is one of the most promising therapeutic approaches to restore neurological function in patients affected by neurodegenerative diseases. Endogenous NSC of the subventricular zone (SVZ) can be selectively targeted by lipid nanocapsules (LNC) coated with the peptide NFLTBS.40-63 (NFL-LNC) after intra-lateral ventricular injection in the brain. NFL-LNC can potentially deliver active compounds to SVZ-NSC and thus promote their differentiation to treat neurodegenerative diseases. The aim of this work was to induce endogenous NSC differentiation by specifically delivering retinoic acid (RA) to SVZ-NSC *via* NFL-LNC. RA was successfully encapsulated into NFL-LNC and RA-NFL-LNC were incubated with primary rat SVZ-NSC. *In vitro*, RA-NFL-LNC decreased the number of nestin$^+$ (NSC marker) cells and neurospheres compared to controls and increased the number of GalC$^+$ (oligodendrocytic marker) cells. Then, RA-NFL-LNC were injected in the right lateral ventricle of a lysolecithin-induced rat focal white matter lesion model to evaluate their impact on oligodendrocyte repopulation and remyelination. RA-NFL-LNC significantly increased the percentage of mature oligodendrocytes, stimulating oligodendrogenesis, nearly to the pre-lesion levels. Thus, RA-NFL-LNC represent a promising nanomedicine to be further investigated in the treatment of demyelinating diseases.

1. Introduction

Central nervous system (CNS) degenerative diseases are a heterogeneous group of disorders characterized by the progressive development of lesions and loss of specialized neural cells such as neurons, astrocytes and oligodendrocytes [1,2]. Oligodendrocytes are myelinating cells which modulate axonal conduction and provide trophic support to neurons [3]. Myelin dysfunction and oligodendrocytic failure are primarily involved in the etiology of many demyelinating CNS diseases (e.g., multiple sclerosis and multiple system atrophy) which have high economic and social costs worldwide [4].

Neural stem cells (NSC) have been investigated to treat such diseases since many studies demonstrated partial neurological function recovery after their transplantation in animal models [5]. NSC are located in restricted neurogenic niches of the CNS (e.g., the central canal of the spinal cord, the subventricular zone (SVZ) and subgranular zone

* Corresponding author. Université catholique de Louvain, Louvain Drug Research Institute, Advanced Drug Delivery and Biomaterials, Avenue E. Mounier 73, Bte 1Brussels, Belgium.
E-mail address: anne.desrieux@uclouvain.be (A. des Rieux).

https://doi.org/10.1016/j.biomaterials.2019.119653
Received 14 August 2019; Received in revised form 15 November 2019; Accepted 24 November 2019

of the brain). The therapeutic effect of NSC is mostly related to their differentiation and proliferation, by which they can replace damaged cells and enhance the recovery of the affected areas [6]. Several NSC-based strategies have been developed to treat CNS diseases, either using exogenous NSC (induced from other somatic cells or isolated from neurogenic niches) or endogenous NSC (niche-localized) [7]. NSC differentiation is aimed to occur either *in vivo* after transplantation of *in vitro* expanded/stimulated exogenous NSC or *in situ* after endogenous NSC stimulation.

In situ differentiation of endogenous NSC is one of the most promising strategies to treat demyelinating diseases as it does not present the issues typically associated with NSC transplantation (i.e. limited access to cell supply, cell viability after transplantation) [8] and *in vitro* manipulations (i.e. risk of contamination and genetic modifications) [9]. Nevertheless, the lack of drugs and delivery systems with the dual property of selectively targeting endogenous NSC (to reduce off-target effects) and stimulating their differentiation has hampered the development of this therapeutic approach.

The peptide NFL-TBS.40–63 (NFL) is a 24-amino acid peptide corresponding to the tubulin-binding site of the neurofilament light subunit [10]. It selectively penetrates SVZ-NSC by direct translocation *in vitro* while it localizes to SVZ-NSC niches after intra-lateral ventricle injection into rat brain *in vivo* [11]. Although NFL targets SVZ-NSC and induces their differentiation into neurons and oligodendrocytes *in vitro* [12], no corresponding effect has yet been described *in vivo*. Moreover, the peptide has a strong structure-activity correlation [13] which limits chemical grafting (i.e. covalent binding) between NFL and either bioactive molecules or vectors to form prodrugs or targeted delivery systems, respectively. Thus, although the direct therapeutic application of the peptide to target and differentiate NSC *in situ* is not excluded, its association with a drug delivery system represents a promising strategy for the selective delivery of bioactive molecules to stimulate SVZ-NSC differentiation.

In our previous work [14], NFL was adsorbed on the surface of lipid nanocapsules [15] (LNC) to confer NSC-targeting properties to LNC. We demonstrated that NFL-LNC interact with primary SVZ-NSC *in vitro* and co-localize with SVZ-NSC after injection in the brain lateral ventricle of rat [14]. The SVZ is one of the most important neurogenic regions of the CNS that is involved in the origin/development of many CNS diseases [16–18]. Thus, targeting SVZ-NSC with NFL-LNC loaded with a pro-differentiation molecule could induce endogenous NSC differentiation.

All-trans-retinoic acid (RA) is a metabolic product of vitamin A that stimulates neural differentiation, axonal outgrowth and neuronal patterning in the developing nervous system [19]. RA is used *in vitro*, alone or in cocktails, to induce neural differentiation of different stem cell populations including NSC [19,20]. However, RA is practically insoluble in aqueous solutions and is subjected to fast degradation in its free form.

To overcome these limitations and achieve the full therapeutic potential of RA, we developed a new nanomedicine where RA is encapsulated in NFL-LNC. We hypothesized that NFL-LNC loaded with RA would specifically target SVZ-NSC and stimulate their endogenous differentiation. We prepared and characterized RA-loaded NFL-LNC (RA-NFL-LNC). Then, the impact of RA-NFL-LNC on NSC differentiation was evaluated *in vitro* on primary SVZ-NSC, and *in vivo* in a rat model of white matter focal demyelination.

2. Materials and methods

2.1. Materials

Biotinylated NFL-TBS.40-63 (NFL) was purchased from GeneCust (Luxembourg, Luxembourg). Labrafac® provided by Gattefosse SA (Saint-Priest, France) and Lipoïd® by Lipoid Gmbh (Ludwigshafen, Germany). Kolliphor HS®, L-α-Lysolecithin, poly-D-Lysine hydrobromide (70000–150000 Da) and retinoic acid were purchased from Sigma (Saint-Louis, Missouri, USA). Sodium chloride (NaCl) was purchased from Prolabo (Fontenay-sous-bois, France). Primary antibodies against galactosylceramidase (GalC), myelin-associated glycoprotein (MAG) and myelin-basic protein (MBP) were purchased from Merck Millipore (Billerica, Massachusetts, USA). Primary antibodies against pan neurofilament (panNF) and βIII tubulin were purchased from Biolegend (San Diego, California, USA). Primary antibodies against nestin and glial fibrillary acid protein (GFAP) were purchased from Abcam (Cambridge, United Kingdom). Primary antibody against oligodendrocyte transcription factor 2 (Olig2) was purchased from Thermo Fisher Scientific (Zaventem, Belgium). Secondary antibodies Alexa 488 anti-mouse, Alexa 488 anti-rabbit, Alexa 594 anti-mouse and Alexa 594 anti-rabbit were purchased from Thermo Fisher Scientific. HEPES, Pen/Strept, Na pyruvate, B27, MEM alpha (no nucleosides), 0.05% trypsin-EDTA (1x), DNAse and ProLong Gold antifade were purchased from Thermo Fisher Scientific. Epidermal growth factor (EGF) was purchased from Peprotech (London, United Kingdom). CellTiter 96® AQueous One Solution Cell Proliferation Assay was purchased from Promega (Fitchburg, Wisconsin, USA). Formaldeyde solution 37% was purchased from Carl Roth (Karlsruhe, Germany). Amicon Ultra-0.5 mL 30 K filters were purchased from Merck Millipore (Billerica, Massachusetts, USA). Rotilabo®-syringe sterile 0.22 µm filters were purchased from Carl Roth GmbH. VECTASHIELD® antifade mounting medium containing DAPI was purchased from Vector Laboratories (Burlingame, California, USA). The isolation of NSC and *in vivo* experiments were performed according to Directive 2010/63/EU, to guidelines of the Belgian Government following the approval by the ethical committee for animal care of the faculty of medicine of UCLouvain (2017/UCL/MD/030).

2.2. Preparation of retinoic acid-loaded NFL-lipid nanocapsules (RA-NFL-LNC)

LNC were prepared following the protocol developed by Heurtault et al. [21]. Briefly, Kolliphor HS15® (0.846 g), Lipoïd® (0.075 g), NaCl (0.089 g), Labrafac® (1.028 g) and water (2.962 g) were mixed under gentle magnetic stirring at 30 °C for 5 min. The solution was progressively heated (90 °C) and cooled (60 °C) three times. During the last cooling, cold water (12.5 g at 4 °C) was added at 72–74 °C under high speed stirring. RA-loaded LNC were prepared by adding 100 µL of RA stock solution (20 mg/mL in DMSO) during the last cooling of LNC preparation (final volume of 15 mL). Alternatively, blank LNC were prepared by adding 100 µL of DMSO. LNC were filtered on 0.22 µm filter and stored at 4 °C until further use. NFL-LNC were produced by incubating 369 µL of 1 mM NFL (in nanopure water) overnight at room temperature (RT) with 1 mL of LNC under gently stirring, while non-targeted LNC were incubated with 369 µL of water [14]. Final concentrations were ~400 µM RA in 126 mg/mL of LNC for RA-LNC and ~400 µM RA, 270 µM NFL in 126 mg/mL of nanoparticles for RA-NFL-LNC.

2.3. Characterization of RA-NFL-LNC

Size, zeta-potential and PDI of nanoparticles were measured using a Malvern Zetasizer Nano ZS (Malvern Instruments) (N = 3). For the measurement of size and PDI, samples were diluted 1/100 (v/v) in water. For the measurement of zeta-potential, samples were diluted 1/100 (v/v) in NaCl 10 mM.

The encapsulation efficiency of RA was calculated by using the following formula:

$$Encapsulation\ Efficiency = \frac{RA\ total - non\ encapsulated\ RA}{RA\ introduced\ in\ the\ formulation} * 100$$

RA total was extracted from RA-LNC by dissolution in methanol at a ratio 1:20 (RA total). Non-encapsulated RA was separated from RA-LNC by ultra-filtration. RA was quantified by Reverse phase-High Liquid

Chromatography (Waters®) with a Macherey-Nagel® 125/4 NUCLEODUR 100-5 C 18 column with a mobile phase composed of water and acetonitrile (15:85 v/v) containing 0.1% TFA. The flow rate was at 1 mL/min in isocratic mode with a volume of injection of 20 µL and the detection wavelength was set at 342 nm.

2.4. Isolation of neural stem cells (NSC)

SVZ-NSC were isolated from new born rat (P7, except otherwise stated) SVZ as previously described [14]. The cells were seeded at 2×10^5 cells/Petri 60 mm in 5 mL of cell culture medium (1.25 mL of D-glucose 1 M, 750 µL of HEPES, 500 µL Pen/Strept, 500 µL NaPyruvate, 500 µL of B27 and 10 ng/mL of EGF in 50 mL of MEM alpha no nucleosides medium). NSC were cultivated as floating neurospheres, which appeared after 5 days, at 37 °C in 5% CO_2. Either floating neurospheres or adherent dissociated cells have been used during this study, depending on the aim of the experiment.

2.5. NSC viability after RA-NFL-LNC incubation

Five days after isolation, neurospheres corresponding to 3×10^5 SVZ-NSC/mL were incubated for 1 h at 37 °C with different dilutions of RA-NFL-LNC stock solution (1/50, 1/100, 1/500 and 1/1000 in PBS) or with different treatments (vehicle, NFL, LNC, NFL-LNC, RA, RA-LNC and RA-NFL-LNC) diluted 1/100 in PBS. Then, neurospheres were washed, dissociated by using a 26 G needle, and seeded at 3×10^5 cells/mL on poly-D-Lysine (0.1 mg/mL in nanopure water) coated 96-well plates. Cell viability was measured after 1 h, 2 days and 7 days using the CellTiter 96® AQueous One Solution Cell Proliferation assay following supplier's instructions (N = 4, n = 3).

2.6. Impact of RA-NFL-LNC on NSC stemness in vitro

Five days after isolation, neurospheres were incubated for 1 h with RA-NFL-LNC or controls (vehicle, NFL, LNC, NFL-LNC, RA, RA-LNC) at a 1/100 dilution as described in 2.5. The impact of RA-NFL-LNC on NSC stemness was determined (i) by counting the number of neurospheres and (ii) by quantifying the percentage of nestin$^+$ cells 2 and 7 days after treatment.

(i) After 1 h-incubation with RA-NFL-LNC or controls, neurospheres were centrifuged, the supernatants containing nanoparticles or molecules that did not interact with the cells were discarded while the neurospheres were resuspended in fresh medium. The number of neurospheres (equivalent to 3×10^5 cells/mL or to 1.5×10^5 cells/mL for evaluation at day 2 and day 7, respectively) was counted manually 2 days (N = 4) and 7 days (N = 3) post-treatment. Results were expressed relative to the control group (untreated neurospheres, set at 100%) at the time of analysis (2 or 7 days). A minimum of 3 pictures/well were analysed.

(ii) Neurospheres were dissociated and seeded on poly-L-Lysine coated 24-well cover-slips at 3×10^5 cells/mL or at 1.5×10^5 cells/mL (for evaluation at 2 days (N = 4) and 7 days (N = 6) post-treatment, respectively). Cells were stained for nestin by overnight incubation with rabbit anti-nestin primary antibody (ab92391, 1/250 in BSA 1%) and with an Alexa 488 anti-rabbit secondary antibody (1/400 in PBS), and mounted with VECTASHIELD® antifade mounting medium containing DAPI. The percentage of nestin$^+$ cells was calculated relative to the total number of cells (ImageJ 1.51j8). A minimum of 3 pictures/cover slip was acquired using an EVOS fluorescent microscope.

2.7. Influence of RA-NFL-LNC on NSC differentiation

Five days after isolation, neurospheres were incubated for 1 h with RA-NFL-LNC or controls (vehicle, NFL, LNC, NFL-LNC, RA and RA-LNC, 1/100 dilution in PBS), dissociated and seeded as described in 2.6 (N = 4 and N = 3 for 2 and 7 days post treatment evaluation, respectively).

Two days after treatment, SVZ-NSC were stained overnight for GFAP and βIII tubulin with a rabbit anti-GFAP primary antibody (ab7779, 1/1000 in BSA 1%) and a mouse anti-βIII tubulin primary antibody (801202, 1/1000 in BSA 1%), followed by 2-h incubation with appropriate secondary antibodies (Alexa 594 anti-rabbit and Alexa 488 anti-mouse (1/400 in PBS), respectively). Seven days after treatment, SVZ-NSC were stained with a mouse anti-pan-NF (SMI-311R-100, 1/1000 in BSA 1%) or a mouse anti-GalC (MAB342, 1/500 in BSA 1%) primary antibody, followed by incubation with appropriate secondary antibody (Alexa 488 anti-mouse and Alexa 594 anti-mouse (1/400 in PBS), respectively). Samples were mounted with VECTASHIELD® antifade mounting medium containing DAPI. A minimum of 3 pictures/cover slip was acquired. The percentages of GFAP$^+$, βIII tubulin$^+$, panNF$^+$ and GalC$^+$ cells were calculated relative to the total number of cells (ImageJ 1.51j8).

2.8. Impact of RA-NFL-LNC on oligodendrocyte repopulation and on remyelination in vivo

Focal demyelination was achieved by adapting a protocol developed by Miron et al. [22]. The lesion was induced in the *corpus callosum* of 2 month-old female Wistar rats (n = 4) by stereotaxic injection (32G) in the right hemisphere (ML: + 2.1; AP: 0.8; DV: + 3) of 2 µL of 1% lysolecithin in PBS (0.5 µL/min) using a Harvard apparatus stereotaxic frame and injector (Holliston, Massachusetts). Three days after lysolecithin injection, 20 µL of RA- NFL-LNC or controls (vehicle, NFL, LNC, NFL-LNC, RA and RA-LNC, no dilution) were injected (0.5 µL/min) into the right lateral ventricle (ML: + 1.5; AP: 0.8; DV: + 4). Five days after treatment (7 days after lesioning), animals were sacrificed by overdose of isoflurane and intracardially perfused with 4% paraformaldehyde in 0.9% NaCl solution. Brains were post-fixed for 6 h in PFA 4% and incubated in 30% sucrose overnight before storage at −80 °C in OCT until further analysis. The injection sites (lysolecithin and treatment) and the area used for image analysis are highlighted in Fig. 1.

Immunofluorescence was performed on 12-µm brain serial sections fixed with cold methanol for 10 min at −20 °C. Sections were then washed 3 times in PBS and incubated with BSA 5% in PBS for 1 h at RT. They were then incubated either with rabbit anti-Olig2 (P21954), or with mouse anti-MAG (MAB1567) and rabbit anti-MBP (AB5864) primary antibodies overnight at 4 °C (1:400 in PBS). Sections were then incubated with appropriate secondary antibodies (Alexa 488 anti-rabbit and Alexa 594 anti-mouse (1:1000 in PBS)) for 90 min at RT. Sections were mounted with VECTASHIELD® antifade mounting medium containing DAPI. A minimum of 3 pictures/section and minimum 3 sections/rat was acquired with an EVOS fluorescent microscope. The percentages of Olig2$^+$, MAG$^+$ and MBP$^+$ staining (number of pixels) were calculated relative to the total surface of the picture (ImageJ 1.51j8).

2.9. Statistical analyses

Statistically significant differences were evaluated using a Mann-Whitney test, one-way ANOVA or two-way ANOVA using Prism 7.00 (GraphPad software, San Diego, CA). Results are expressed as mean ± SEM and were considered significant if $p < 0.05$. N refers to the number of independent experiments. In figure captions, detailed information about number of replicates, statistical test and post-test can be found for each experiment.

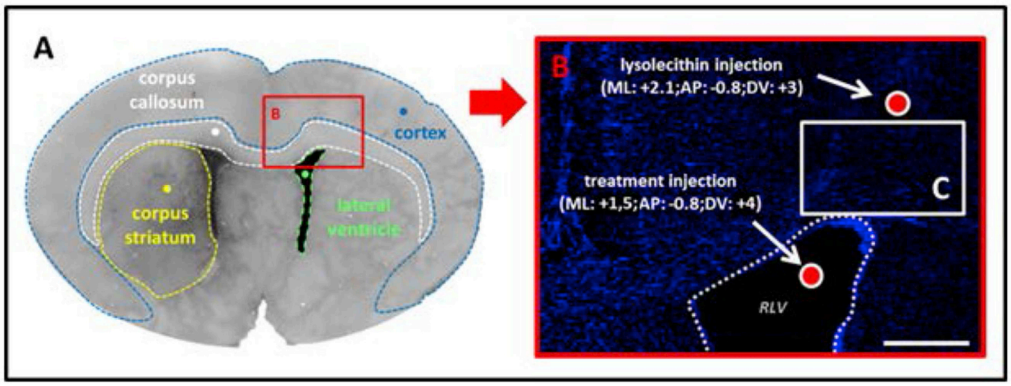

Fig. 1. Areas of the brain where injections and image analysis were performed. A) Coronal brain section highlighting the main compartments of the brain and the zone where the experiment was performed. B) Injection sites (RLV: right lateral ventricle). Scale bar: 500 μm. C, area subjected to image analysis.

3. Results

3.1. RA-NFL-LNC physico-chemical properties

To assess the impact of RA encapsulation on LNC physicochemical properties, size, polydispersity index (PDI) and zeta-potential of RA-NFL-LNC were measured and compared to controls (LNC, NFL-LNC and RA-LNC). Addition of RA to the formulations (+/− NFL) did not influence LNC characteristics but tended to slightly increase the PDI (to 1.4–3.5-folds) and to decrease the zeta-potential (to 1.3–1.9-folds) (Fig. 2A). NFL adsorption at LNC surface increased size, PDI and zeta-potential as previously observed [14]. RA encapsulation efficiency was 87.6% (Fig. 2B), allowing to reach ~ 400 μM of RA.

3.2. RA-NFL-LNC do not impact SVZ-NSC viability in vitro

The aim was to evaluate the impact of RA-NFL-LNC on SVZ-NSC viability and identify a range of non-cytotoxic working concentrations. After 1 h of incubation with RA-NFL-LNC no significant effect was observed on cell viability whatever the concentration (Fig. 3A). Two and seven days after 1 h treatment, cell viability was still 100%. No impact on viability was observed up to 7 days after treatment at a 1/100 dilution (Fig. 3B). For the following experiments, the LNC stock solutions were diluted at 1/100 (1.26 mg/mL final) [14,23]. As 1 h of RA-NFL-LNC incubation with neurospheres, and their subsequent dissociation, did not affect SVZ-NSC viability, these conditions were consequently deemed appropriate for the following *in vitro* differentiation experiments.

Results were expressed related to non-treated cells (vehicle, red dotted line). N = 4, Two-way ANOVA, Dunnett's multiple comparison test among all groups. $p > 0.05$.

3.3. RA-NFL-LNC reduce SVZ-NSC stemness in vitro

The objective of this experiment was to evaluate the effect of RA-NFL-LNC on NSC stemness. Self-renewal is the ability of stem cells to proliferate by maintaining an undifferentiated state and its loss typically accompanies stem cell differentiation into specialized cells [24]. Readouts were performed 2 days after treatment, since morphological modifications were observed by bright-field microscopy, and at 7 days post treatment, since it is one of the most commonly used time-point in the literature for this purpose [25,26]. Indicators of self-renewal are NSC ability to form floating neurospheres and expression of nestin. The evaluation was performed by neurosphere counting and nestin$^+$ cell quantification.

The impact on the number of neurospheres formed after 1 h SVZ-NSC incubation following treatment with RA-NFL-LNC was first evaluated. The percentage of neurospheres that remained in suspension 2 days after treatment, when compared to untreated control, decreased following exposure to RA-NFL-LNC but also to RA, NFL, and NFL-LNC (Fig. 4A, left, and Supplementary Data, Fig. 1S). After 7 days, the percentage of neurospheres vs untreated control decreased when cells were incubated with RA-NFL-LNC, NFL and NFL-LNC (Fig. 4A, right, and Supplementary Data, Fig. 1S).

The influence on nestin$^+$ cells of SVZ-NSC following incubation with RA-NFL-LNC was also investigated. Neurospheres were incubated for 1 h with RA-NFL-LNC or under control conditions, and were dissociated 2 and 7 days later (adherent cultures). Incubation with RA-NFL-LNC and NFL-LNC significantly decreased the number of nestin$^+$ cells 2 and 7 days after treatment when compared to untreated control (Fig. 4B and Supplementary Data, Fig. 2S).

3.4. RA-NFL-LNC stimulate SVZ-NSC differentiation in vitro

To evaluate the effect of RA-NFL-LNC on *in vitro* SVZ-NSV

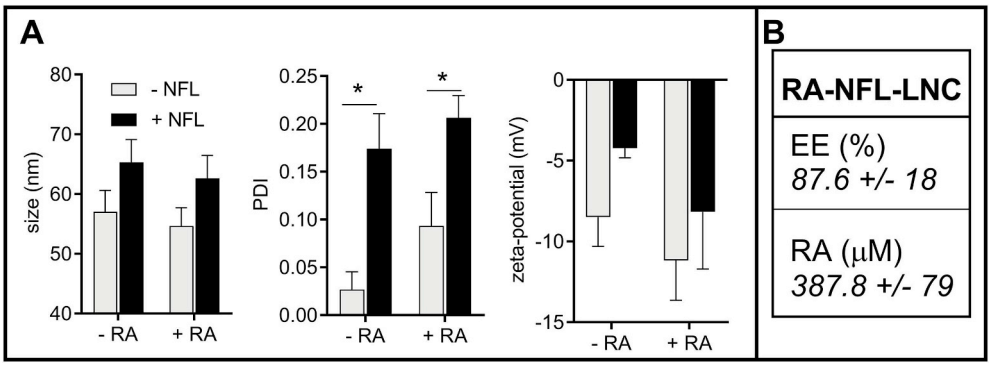

Fig. 2. Physiochemical characteristics of RA-NFL-LNC. A) Size, PDI and zeta-potential were measured by diluting the nanoparticles 1/100 (v/v) in water (size and polydispersity index, PDI) or in NaCl 10 mM (zeta-potential). N = 3, two-way ANOVA with Bonferroni's post-hoc test, *$p < 0.05$. B) RA encapsulation efficiency (EE%) and concentration (μM) in RA-NFL-LNC.

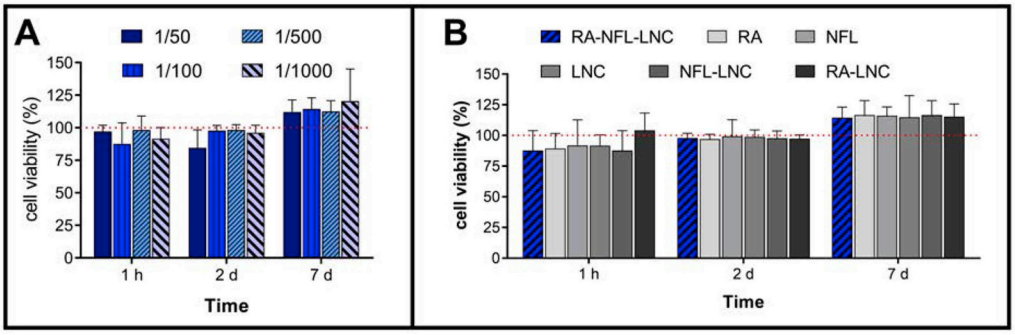

Fig. 3. RA-NFL-LNC do not impact NSC viability. A) SVZ-NSC viability was evaluated directly (1 h), 2 days (2 d) and 7 days (7 d) after 1 h incubation with RA-NFL-LNC by MTS at different dilutions (1/50, 1/100, 1/500 and 1/1000 corresponding to 8 μM RA-5.4 μM NFL-2.52 mg/mL, 4 μM RA-2.7 μM NFL-1.26 mg/mL, 0.8 μM RA-0.54 μM NFL-0.252 mg/mL and 0.4 μM RA-0.27 μM NFL-0.126 mg/mL, respectively) of the stock solution. B) Viability of SVZ-NSC was evaluated after 1 h incubation with RA-NFL-LNC (4 μM RA-2.7 μM NFL-1.26 mg/mL) and all controls at a 1/100 dilution.

differentiation into specialized neural cells (i.e., neurons, astrocytes or oligodendrocytes), specific markers were used to stain treated cells 2 and 7 days after incubation with RA-NFL-LNC or the controls. These time points have been selected using the same rational as explained in 3.3. The influence of RA-NFL-LNC on early NSC differentiation was first investigated by staining cells 2 days after treatment with a marker of astroglial and of early neuronal differentiation (GFAP and βIII Tubulin, respectively). The percentage of $GFAP^+$ and βIII $Tubulin^+$ cells significantly increased when cells were treated with RA-NFL-LNC and with NFL compared to untreated control (+26 and +39%, and +22 and +23%, respectively) (Fig. 5). $GFAP^+$ cells increased by 13% when treated with RA-NFL-LNC compared to NFL but not significantly.

The impact of RA-NFL-LNC on NSC differentiation at a later time point (7 days after treatment) was then studied using astrocyte (GFAP), oligodendrocyte (galactosylceramidase, GalC) and neuronal markers (pan-neurofilament, panNF) following the same protocol as for the early differentiation. The percentage of $GalC^+$ cells significantly increased (+23%) after incubation with RA-NFL-LNC but not with the other treatments (Fig. 6A). SVZ-NSC treated with RA-NFL-LNC demonstrated a morphology similar to immature oligodendrocytes 7 days after treatment (Fig. 6B). No significant variation was observed in the expression of GFAP and panNF in all treatment conditions ($p > 0.05$) (data not shown). However, the extent of oligodendrocyte differentiation was influenced by RA-NFL-LNC concentration (Fig. 6C).

To determine whether the NSC response to RA-NFL-LNC was dependent on the state of NSC (i.e. to compare younger more plastic cells with older more mature cells), SVZ-NSC were isolated from 7-day old and 2-month old rats, treated with RA-NFL-LNC and assessed for GalC expression 7 days after treatment. No significant impact of NSC age on oligodendrocyte differentiation was observed (Supplementary Data, Fig. 3S).

3.5. RA-NFL-LNC supports oligodendrogenesis in vivo

Given that RA-NFL-LNC were found to stimulate NSC differentiation into oligodendrocytes, we then investigated whether this formulation could enhance oligodendrogenesis *in vivo* following myelin damage. We used a focal lesion model whereby we stereotaxically injected the myelin toxin lysolecithin into the *corpus callosum*, a white matter tract in proximity to the SVZ where NSC differentiation into

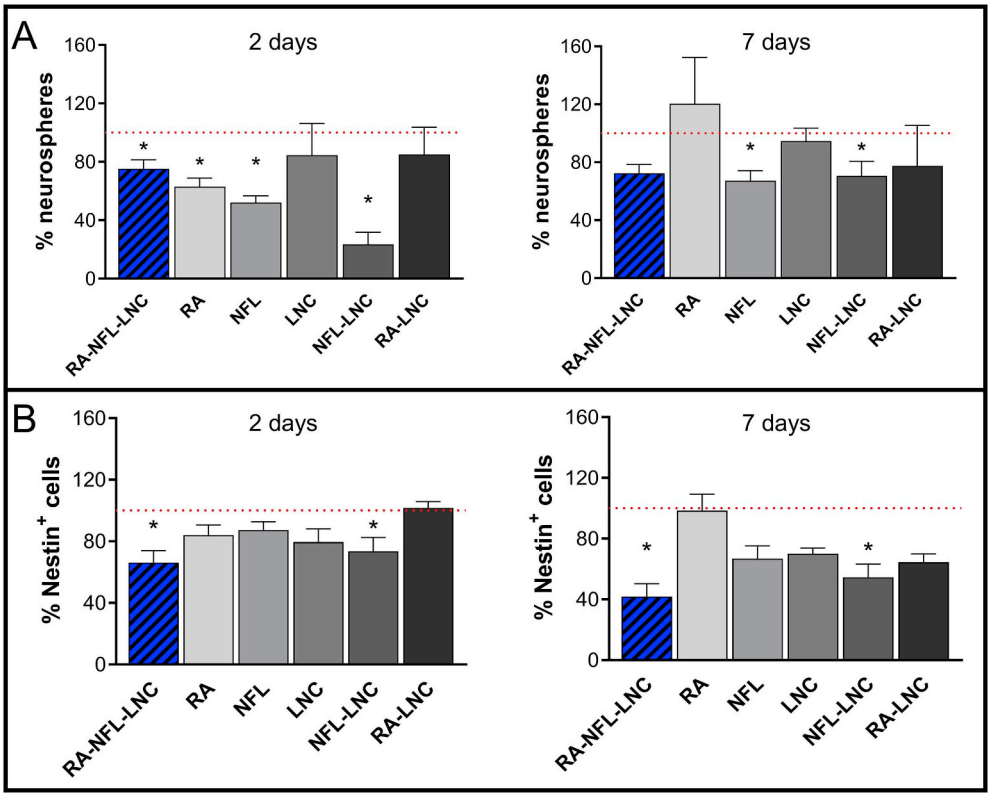

Fig. 4. RA-NFL-LNC reduce SVZ-NSC stemness. A) Number of neurospheres at 2 (left) and 7 (right) days after treatment of SVZ-NSC with RA-NFL-LNC or controls for 1 h (red dotted line: number of neurospheres in control conditions). B) Percentage of $nestin^+$ cells at 2 (left) and 7 (right) days after treatment of SVZ-NSC with RA-NFL-LNC or controls for 1 h and dissociated before seeding, (red dotted line: percentage of $nestin^+$ in untreated NSC cultures). N = 4 (A) and N = 3 (B), One-way ANOVA, Dunnett's multiple comparison test versus vehicle, *$p < 0.05$. (For interpretation of the references to colour in this figure legend, the reader is referred to the Web version of this article.)

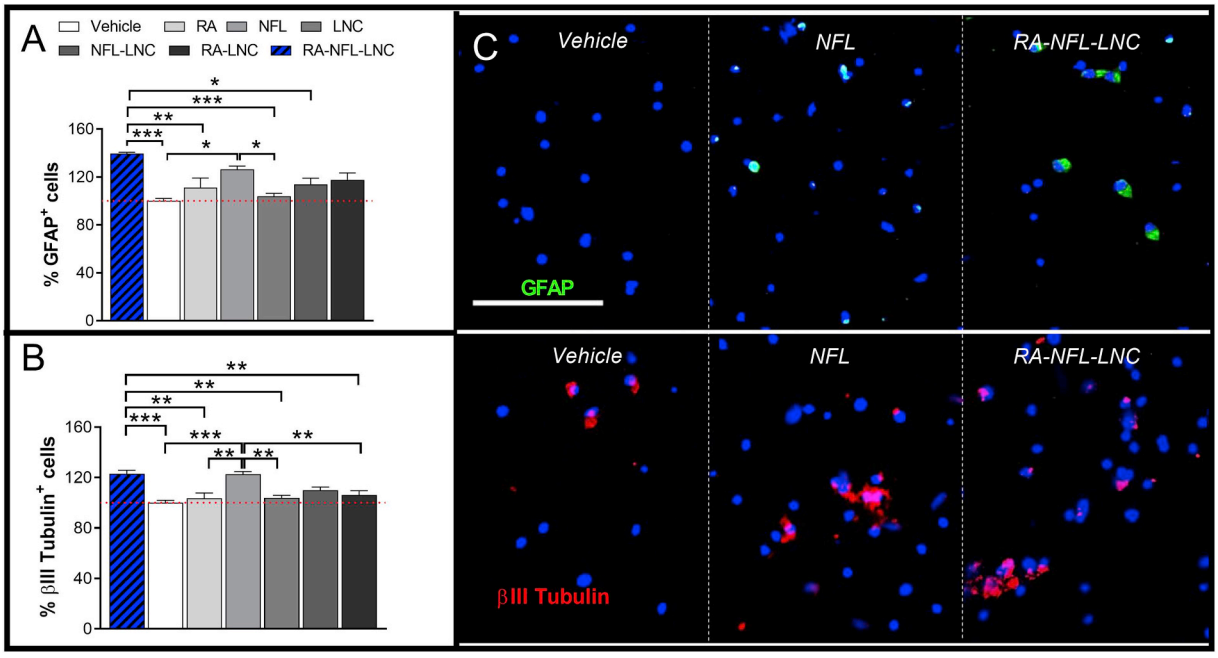

Fig. 5. RA-NFL-LNC stimulate SVZ-NSC early differentiation. SVZ-NSC were incubated for 1 h with RA-NFL-LNC or controls and dissociated before seeding. Two days after treatment, cells were immunostained for A) GFAP (marker of astroglial differentiation) and B) βIII Tubulin (early marker of neuronal differentiation). The percentage GFAP$^+$ or βIII Tubulin$^+$ cells in untreated NSC was considered to be 100% (red dotted line). N = 4, One-way ANOVA, Dunnett's multiple comparison test versus vehicle, *p < 0.05, **p < 0.01, ***p < 0.001. C) Representative images of SVZ-NSC immunostaining immunostained for GFAP (green), βIII Tubulin (red) and DAPI (nucleus, blue) 2 days after 1 h of treatment. Scale bar: 100 μm.

oligodendrocytes has previously been observed.

Lysolecithin injection induced focused demyelination, by destructuring the myelin sheath (surfactant effect) and, consequently, death of oligodendrocytes. It does not attempt to accurately mimic demyelinating diseases with complex etiology and pathogenesis (such as multiple sclerosis) but it is a well-known model for proof-of-concept studies aiming at investigating a specific aspect of a complex pathology. The lesion is physiologically and fully recovered by the animals at various rates, depending of the initial lysolecithin concentration and the animal species [27].

RA-NFL-LNC were injected into the lateral ventricle directly below the lesion site (Fig. 1).

The percentage of oligodendrocyte lineage cells (Olig2$^+$) significantly decreased in the zone of interest after lysolecithin injection (−79% vs Sham) (Supplementary Data, Table 1S).

Injection of RA-NFL-LNC and RA-LNC resulted in +50% of Olig2$^+$ population recovery vs vehicle-treated animals (PBS) to reach 70% of the original population (versus sham) (Fig. 7).

Then, the influence of RA-NFL-LNC on remyelination was evaluated by quantification of MAG$^+$ and MBP$^+$ cells (early and late stage myelination markers, respectively). As observed for Olig2$^+$ cells, the percentage of MBP$^+$ and MAG$^+$ cells significantly decreased after lysolecithin injection (to −69 and −58% of Sham, respectively) (Supplementary Data, Table 1S). Treatment with RA-NFL-LNC and RA-LNC significantly increased the percentage of MBP$^+$ and MAG$^+$ cells compared to vehicle-treated animals (PBS), similar to levels in sham

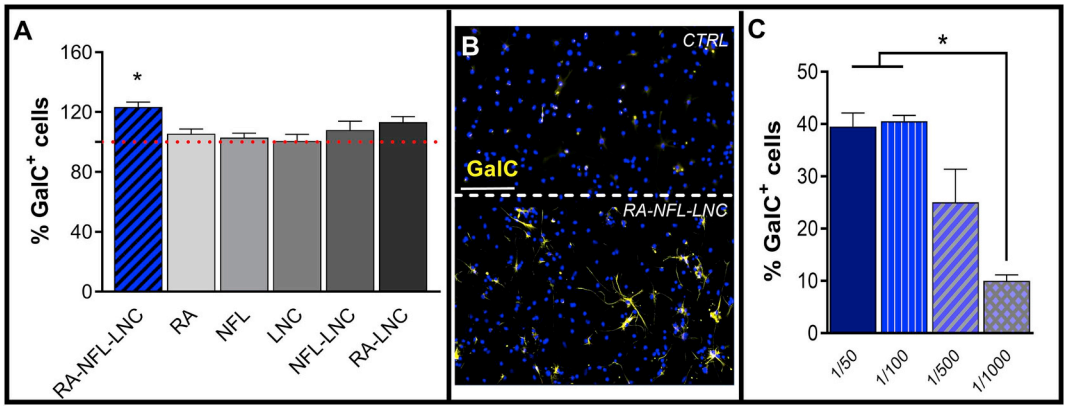

Fig. 6. RA-NFL-LNC promote SVZ-NSC differentiation into oligodendrocytes. A) Percentage of SVZ-NSC positive for oligodendrocyte marker GalC at 7 days after treatment for 1 h with RA-NFL-LNC and controls (red dotted line: untreated control). N = 4, One-way ANOVA, Bonferroni's multiple comparison test amongst all groups. *p < 0.05. B) representative images of SVZ-NSC immunostained for DAPI (nucleus, in blue) and GalC (yellow) after 1 h treatment with RA-NFL-LNC or without treatment (CTRL). Scale bar: 100 μm. C) Impact of RA-NFL-LNC concentration on NSC differentiation toward the oligodendrocyte lineage. GalC expression was evaluated after 1 h incubation of 7-days old SVZ-NSC with RA-NFL-LNC at different dilutions (1/50, 1/100, 1/500 and 1/1000). Cells were immunostained for GalC. N = 3, One-way ANOVA, Tukey's multiple comparison test, *p < 0.05. (For interpretation of the references to colour in this figure legend, the reader is referred to the Web version of this article.)

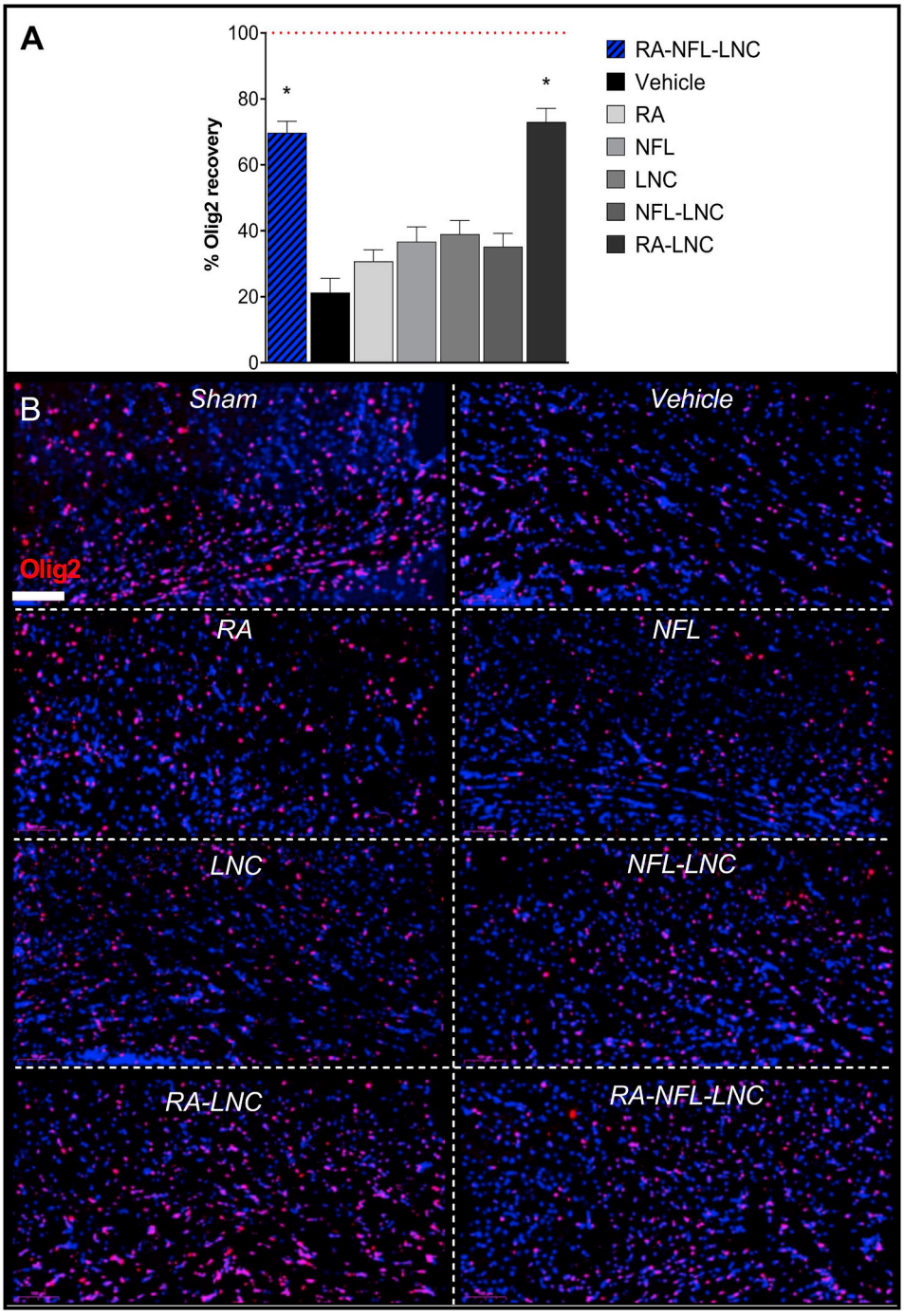

Fig. 7. RA-NFL-LNC allow oligodendrocyte repopulation after lysolecithin-induced focal lesion. A) Five days after treatment, Olig2^{+} cells were quantified by immunostaining. The results are expressed as the percentage of recovery of each population compared to non-lesioned animals (Sham). The negative control was vehicle-treated animals (PBS). N = 4, One-way ANOVA, Dunnett's multiple comparison test relative to vehicle, *p < 0.05. B) Representative pictures of immunostained brain sections for DAPI (nucleus, in blue) and Olig2 (red). Scale bar: 100 μm. (For interpretation of the references to colour in this figure legend, the reader is referred to the Web version of this article.)

controls (Fig. 8).

4. Discussion

The burden of neurodegenerative diseases is steadily increasing and no curative treatment is currently available. One potential therapeutic strategy would be to obtain new neural cells to replace the ones affected by disease. Most ongoing clinical trials relating to NSC used exogenous NSC transplantation, as NSC can be differentiated into mature neural cell types. The therapeutic potential of NSC differentiation is attested by many exogenous NSC differentiation-based therapies to treat CNS diseases that are under clinical trials (e.g., NCT01772810 for spinal cord injury, NCT03309514 for Parkinson's disease, NCT03005249 for cerebral palsy) but efficacy, safety and long-term outcome have yet to be confirmed prior to large-scale therapeutic applications. An alternative strategy that could potentially accelerate the development of NSC differentiation-based therapies and avoid many of the issues associated with exogenous NSC-based approaches (e.g., limited access to cell supply, cell viability after transplantation), is to stimulate endogenous NSC differentiation locally *in situ*. Unfortunately, this remains a challenge due to the lack of dual NSC targeting/differentiating therapies and the challenging translation from *in vitro* to *in vivo* application. Our objective was to promote endogenous NSC differentiation following brain injury by delivering an active molecule *via* NSC-targeted nanocapsules. We have shown that retinoic acid-loaded NFL-functionalized lipid nanocapsules (RA-NFL-LNC) stimulate NSC differentiation towards the oligodendrocyte lineage *in vitro*, and promoted oligodendrogenesis following brain injury *in vivo*.

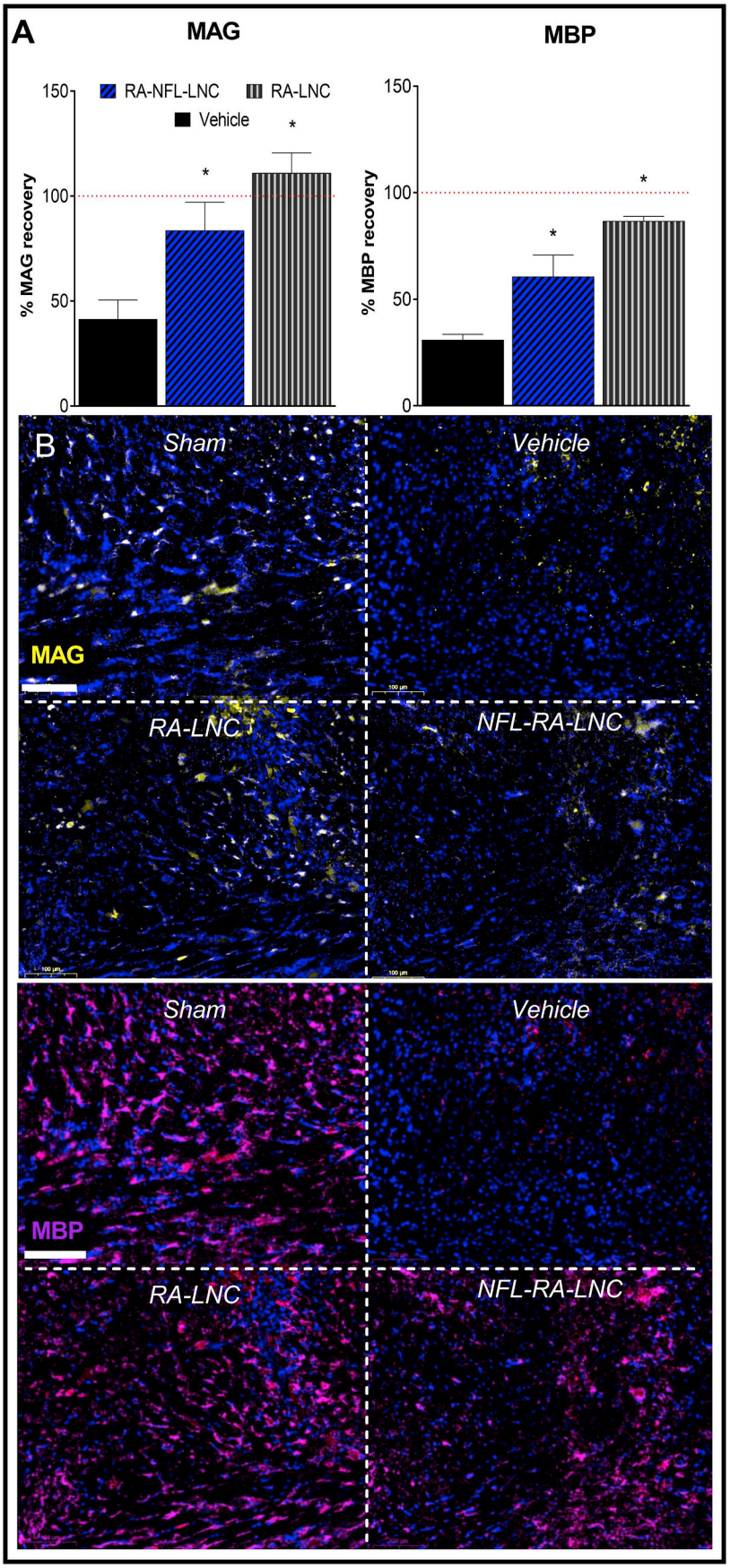

Fig. 8. RA-NFL-LNC stimulate oligodendrogenesis after lysolecithin-induced focal demyelination. A) Five days after treatment, MBP^+ and MAG^+ cells were quantified by immunostaining. The results are expressed as the percentage of recovery of each population compared to non-lesioned animals (Sham). The negative control was vehicle-treated animals (PBS). N = 4, one-way ANOVA, Dunnett's multiple comparison test relative to vehicle, *p < 0.05. B) Representative pictures of immunostained brain sections for DAPI (nucleus, in blue), MBP (violet) and MAG (yellow). Scale bar: 100 μm. (For interpretation of the references to colour in this figure legend, the reader is referred to the Web version of this article.)

RA encapsulation in LNC (+/− NFL) did not significantly impact LNC physicochemical characteristics. The PDI increased but remained below 0.2. The high EE (87.6%) was already observed for other lipophilic molecules (e.g., amiodarone [28], paclitaxel [29] and ferrociphenol [30]) and was most likely due to the higher affinity of RA with the LNC oily core (Labrafac®) than with the aqueous phase. Size, PDI and zeta-potential increased after NFL adsorption on LNC surface, as observed in our previous study [14]. We were then able to obtain a targeted nanomedicine loaded with a RA concentration close to 400 μM, suitable to perform *in vitro* and *in vivo* experiments. Compared to other RA-loaded nanoparticle-based formulations [25,31–33], RA-NFL-LNC have a smaller size (up to 10-fold), a less negative zeta-potential (up to 4-fold) and a similar PDI (0.1–0.2) and EE (≈90%).

RA-NFL-LNC concentrations for *in vitro* experiments were chosen in a range where the individual components (RA, NFL, LNC, and NFL-LNC) have not previously shown significant toxicity [14,34]. As expected, RA-NFL-LNC had no major impact on short- and long-term NSC viability at any tested concentration. This excludes cell death-related artefacts in the interpretation of *in vitro* studies.

Important *in vitro* NSC properties such as the capacity to form neurospheres [35] and to express nestin [36], as well as the expression of specialized neural cell markers, are indicators of the balance between proliferation and differentiation. Consequently, the reduction of neurosphere number and nestin expression were indicators of SVZ-NSC transition from an undifferentiated to a differentiating state. The evaluation of these characteristics was performed at an early and late time point (2 and 7 days, respectively). On one hand, as morphological modifications were visible as early as 2 days after treatment, it was important to assess the impact of our nanomedicines at that early stage. On the other hand, 7 days after treatment is the most frequently used time-point to detect NSC differentiation in the literature. It was then selected for the later stage evaluation. Only RA-NFL-LNC and NFL-LNC significantly decreased NSC stemness markers at early and late time points. RA had an effect on neurosphere number only at day 2, LNC had no impact while NFL decreased neurosphere number at day 2 and 7. It seems reasonable to suggest that the impact of RA-NFL-LNC on NSC stemness was due to NFL-LNC rather than RA, even if a synergetic effect between the nanomedicine components was not excluded as the results obtained with their combination differ from the simple addition of each single component. Moreover, the impact of RA on stem cell differentiation can be synergistically modulated by Wnt molecules [37,38]. In fact, cell penetrating peptides as well as fatty acids have been associated with Wnt/β-catenin signaling inhibition and upregulation [39], respectively. Consequently, since NFL is a cell-penetrating peptide and Labrafac (LNC oily core) is a fatty acid, we could thus speculate that they can modulate Wnt signaling and, consequently, synergistically modulate RA impact on NSC differentiation.

We thus investigated the effect of RA-NFL-LNC on NSC differentiation along several neural lineages at these times. Two days after treatment with RA-NFL-LNC, we observed early differentiation of the NSC pool as indicated by increased GFAP and βIII Tubulin, and later differentiation towards the oligodendrocyte lineage as indicated by GalC expression. Although NFL increased the expression of the early markers, it did not induce NSC differentiation into a specific lineage. Interestingly, only the presence of the NSC-targeting peptide NFL at the surface of the RA-loaded LNC allowed NSC differentiation (+10–22%), as no effect was seen for RA or RA-LNC. Co-incubation of RA-LNC and NFL has not been tested, consequently, we could not exclude additive or synergistic effect between NFL and RA-LNC. However, previous studies clearly showed that NFL enhances LNC penetration into NSC (≈6-fold) [14]; it is thus likely that the higher efficiency of RA-NFL-LNC is mostly due to the targeting property of the system. Interestingly, the same increase of $GalC^+$ cells was observed for NSC isolated from young rats (7 days-old) than for older rats (2 months-old), meaning that RA-NFL-LNC pro-differentiating potential also applies to less plastic adult cells. This would positively impact the therapeutic potential of our formulation.

Several examples of RA-loaded drug delivery systems have been successfully applied to different cell types in order to induce their differentiation for therapeutic purposes (e.g., T cell [40], spinal cord oligodendrocyte progenitor cells [41], corneal epithelial cells [42]). Nevertheless, the comparison between RA-NFL-LNC and formulations designed to target endogenous NSC and to stimulate NSC differentiation simultaneously is very limited. According to our knowledge, the only comparable formulation (polyelectrolyte nanoparticles) was designed by Bernardino et al. where RA-loaded nanoparticles (RA^+-NP) successfully stimulated NSC differentiation into the neuronal lineage *in vitro* after 7 days of incubation [25]. RA-NFL-LNC induced a significant effect for a much shorter incubation time even if the physico-chemical characteristics of the vector and the targeted application (neurogenesis versus oligogenesis) were different. As the delivery of the same active compound (RA) induced NSC differentiation in different cell types (neurons and oligodendrocytes), it is quite likely that the formulation used to deliver it has an important role in the preferential orientation of NSC differentiation, *via* additive or synergistic effects. Some lipids are well-known modulators of stem cell proliferation and differentiation [43]. It is thus possible that the lipidic components of RA-NFL-LNC might play a role in the *in vitro* differentiating process which would worth to be elucidated by further investigations. It would thus be interesting to explore the potential complementary effect of those two nanomedicines on neurodegenerative demyelinating diseases like MS.

Oligodendrogenesis stimulation has recently been achieved via physical approaches (e.g., electroacupuncture [44], magnetic stimulation [45], focused ultrasounds [46]) as well as via the delivery of active compounds to oligodendrocyte progenitor cells (OPC). The latest, together with genetic manipulation [47,48], represents the most investigated strategy during the last decade to induce therapeutic oligodendrogenesis. For instance, Rittchen et al. [49] delivered leukaemia inhibitory factor to OPC by poly (lactic-co-glycolic acid) nanoparticles which induced significant oligodendrogenesis and remyelination after focal demyelination. Similarly, Zhang et al. [50] showed that IL-4 nanoparticles improved white matter integrity and attenuated motor/cognitive deficits after stroke by stimulating OPC maturation. The aim of this work was to pursue the novel approach of inducing therapeutic oligodendrogenesis via endogenous NSC differentiation using a versatile NSC-targeting nanomedicine loaded with RA. To investigate the impact of RA-NFL-LNC on *in vivo* oligodendrogenesis following injury, we induced focal demyelinated lesions close to the NSC niche (lateral ventricle) to facilitate differentiation of migrating SVZ-NSC. The treatments were administered 3 days after lysolecithin injection, when demyelination is complete [51], as our objective was to evaluate the effect on oligodendrogenesis (post-lesion) rather than to antagonise the demyelination process. In order to allow time for the treatment to have an effect, we analysed the lesions 5 days later, at 7 days after lysolecithin injection [52]. The aim of the *in vitro* experiment was to ascertain the potential neural phenotypes into which NSC could differentiate by using specific cellular markers. Two days after treatment, βIII tubulin and GFAP were used to investigate early NSC differentiation towards immature neural [53] and astroglial [54] lineages, respectively. Seven days after incubation, panNF, GFAP and GalC were used to study late NSC differentiation towards neurons [55], astrocytes [56] and oligodendrocytes [57], respectively. In order to better discriminate between these last two lineages, treated cells were co-stained for GFAP and GalC, revealing that 7 days after RA-NFL-LNC incubation the number of GFAP + and GFAP+/GalC + cells were not significantly impacted while the number of GalC + cells significantly increased. Since we observed that incubation of RA-NFL-LNC with SVZ-NSC induced their differentiation toward the oligodendrocyte lineage, we focused the *in vivo* experiment on oligodendrogenesis. In order to study the impact of RA-NFL-LNC on oligodendrocyte repopulation, regardless of their maturation, we used Olig2 while, to investigate whether these oligodendrocytes were mature, we used the late differentiation markers MAG and MBP [58]. Five

days after a single injection of either RA-NFL-LNC or RA-LNC into the lateral ventricle, the oligodendrocyte population ($Olig2^+$) significantly increased up to 70% of the original population (versus 20% for the vehicle-treated lesions) while no significant effect was observed for the other treatments. This coincided with increased MAG and MBP positive oligodendrocytes. This study focused on oligodendrogenesis. Further investigations would be required to determine whether this increased oligodendrogenesis translates into increased remyelination. These results demonstrate the strong therapeutic potential of RA-NFL-LNC, as a single injection was found to restore the oligodendrocyte population after demyelination almost to its full extent. On the other hand, the beneficial effect of NFL grafting (i.e., SVZ-NSC targeting) on RA-LNC observed *in vitro* was not visible *in vivo*. In fact, injection of RA-LNC revealed a similar therapeutic effect compared to RA-NFL-LNC but, in principle, this would be achieved via a different mechanism than NSC-differentiation. Although we previously showed that, without NFL functionalization, nanoparticles do not accumulate in SVZ-NSC *in vivo*, excluding any significant impact on NSC-differentiation, the fate of non-targeted LNC is unknown. We hypothesize that untargeted diffusion within cerebrospinal fluid and brain parenchyma occured and allowed non-functionalized nanoparticles to support/promote oligodendrocyte repopulation via pathways other than NSC differentiation. We thus cannot exclude that interactions between RA-LNC and other immature cell types could lead to oligodendrogenesis, nor that impact on inflammation may have played a role. For instance, RA-LNC could interact with NG2-expressing cells (i.e., OPC), which are known to mature into oligodendrocytes [59], and promote a faster oligodendrocyte repopulation compared to RA-NFL-LNC via SVZ-NCS differentiation, avoiding the NSC-to-OPC conversion step [60]. Additionally, LNC could be internalized by microglia, as already shown in our previous work [61] and, via the delivery of RA, they could promote anti-inflammatory responses and support oligodendrogenesis [62]. However, further studies are needed to identify the cells and the mechanisms underpinning non–NSC–targeted RA-LNC effect on oligodendrocyte repopulation and remyelination.

These studies showed that RA-NFL-LNC can significantly promote recovery of the mature oligodendrocyte population after demyelination, demonstrating the therapeutic potential in the scope of demyelinating diseases. Our results are in line with previously reported studies showing *in vitro* NSC differentiation towards the oligodendrocyte lineage after RA incubation [57,63] and *in vivo* endogenous NSC differentiation following intraventricular injection of active compounds [64,65]. We propose that RA-NFL-LNC have the potential to be translated into therapy for the treatment of these diseases. Nevertheless, the intracellular mechanism by which RA-NFL-LNC induce NSC differentiation towards the oligodendrocyte lineage, as well as the study of *in vivo* NSC-differentiating cell migration from the SVZ to the lesion site remain to be elucidated.

5. Conclusion

For the first time, we show that a versatile nanomedicine with the dual property of NSC targeting/differentiation can be successfully applied *in vitro* and *in vivo* for therapeutic purposes. RA-NFL-LNC can penetrate SVZ-NSC and induce their differentiation toward the oligodendrocyte lineage *in vitro*, and, by accumulating in the SVZ-NSC niche, stimulate oligodendrogenesis in a rat focal brain demyelinated lesion after only one injection. RA-NFL-LNC is a promising nanomedicine with a high therapeutic potential for CNS diseases. To further increase its translational value, less invasive routes of administration will be investigated in future. Although intravenously injected LNC do not accumulate in the CNS in significant amounts, surface functionalization with specific BBB-crossing ligands (i.e., transferrin antibody) or the combined use of BBB-permeabilizing physical techniques (i.e., focused ultrasound) could allow therapeutic RA-NFL-LNC dose accumulation in the brain, as shown with other lipid-based nanomedicines. Another alternative administration that could be successfully explored with RA-NFL-LNC is the nose-to-brain route.

Data availability

All the data is available upon request.

CRediT authorship contribution statement

Dario Carradori: Conceptualization, Validation, Investigation, Writing - original draft, Visualization. **Yasmine Labrak:** Investigation, Validation. **Véronique E. Miron:** Methodology, Conceptualization, Writing - review & editing. **Patrick Saulnier:** Writing - review & editing, Supervision, Funding acquisition, Project administration. **Joël Eyer:** Writing - review & editing, Supervision, Project administration. **Véronique Préat:** Writing - review & editing, Supervision, Funding acquisition, Project administration. **Anne des Rieux:** Conceptualization, Validation, Visualization, Writing - review & editing, Supervision, Funding acquisition, Project administration, Funding acquisition.

Acknowledgment

Dario Carradori was supported by NanoFar “European Doctorate in Nanomedicine” EMJD program funded by EACEA. This work was supported by grants from the UClouvain (Fonds Speciaux de Recherche, F.S.R). Anne des Rieux is a F.R.S.-FNRS (Fonds National de la Recherche Scientifique) Senior Research Associate. Anne des Rieux was recipient of a grant from the International Foundation for Research in Paraplegia [P155]. The authors would like to thank Bernard Ucakar and Kevin Vanvarenberg for their precisous help with the animal experiment. In memory of a beloved friend, Françoise Lemoine, who died from MS.

Appendix A. Supplementary data

Supplementary data to this article can be found online at https://doi.org/10.1016/j.biomaterials.2019.119653.

References

[1] K.I. Vadakkan, Neurodegenerative disorders share common features of “loss of function” states of a proposed mechanism of nervous system functions, Biomed. Pharmacother. 83 (2016) 412–430.
[2] K.J. Barnham, C.L. Masters, A.I. Bush, Neurodegenerative diseases and oxidative stress, Nat. Rev. Drug Discov. 3 (2004) 205–214.
[3] U. Fünfschilling, L.M. Supplie, D. Mahad, S. Boretius, A.S. Saab, J. Edgar, B.G. Brinkmann, C.M. Kassmann, I.D. Tzvetanova, W. Möbius, Glycolytic oligodendrocytes maintain myelin and long-term axonal integrity, Nature 485 (2012) 517.
[4] B. Ettle, J.C. Schlachetzki, J. Winkler, Oligodendroglia and myelin in neurodegenerative diseases: more than just bystanders? Mol. Neurobiol. 53 (2016) 3046–3062.
[5] S.K. Vishwakarma, A. Bardia, S.K. Tiwari, S.A. Paspala, A.A. Khan, Current concept in neural regeneration research: NSCs isolation, characterization and transplantation in various neurodegenerative diseases and stroke: a review, J. Adv. Res. 5 (2014) 277–294.
[6] W. Murrell, E. Palmero, J. Bianco, B. Stangeland, M. Joel, L. Paulson, B. Thiede, Z. Grieg, I. Ramsnes, H.K. Skjellegrind, S. Nygard, P. Brandal, C. Sandberg, E. Vik-Mo, S. Palmero, I.A. Langmoen, Expansion of multipotent stem cells from the adult human brain, PLoS One 8 (2013) e71334.
[7] D. Carradori, J. Eyer, P. Saulnier, V. Preat, A. des Rieux, The therapeutic contribution of nanomedicine to treat neurodegenerative diseases via neural stem cell differentiation, Biomaterials 123 (2017) 77–91.
[8] C.A. Herberts, M.S. Kwa, H.P. Hermsen, Risk factors in the development of stem cell therapy, J. Transl. Med. 9 (2011) 29.
[9] O.E. Simonson, A. Domogatskaya, P. Volchkov, S. Rodin, The safety of human pluripotent stem cells in clinical treatment, Ann. Med. 47 (2015) 370–380.
[10] A. Bocquet, R. Berges, R. Frank, P. Robert, A.C. Peterson, J. Eyer, Neurofilaments bind tubulin and modulate its polymerization, J. Neurosci. 29 (2009) 11043–11054.
[11] C. Lépinoux-Chambaud, K. Barreau, J. Eyer, The neurofilament-derived peptide NFL-TBS. 40-63 targets neural stem cells and affects their properties, Stem cells Transl. Med. 5 (2016) 901–913.
[12] C. Fressinaud, J. Eyer, Neurofilament-tubulin binding site peptide NFL-TBS.40-63

increases the differentiation of oligodendrocytes in vitro and partially prevents them from lysophosphatidyl choline toxiciy, J. Neurosci. Res. 92 (2014) 243–253.
[13] R. Berges, J. Balzeau, M. Takahashi, C. Prevost, J. Eyer, Structure-function analysis of the glioma targeting NFL-TBS.40-63 peptide corresponding to the tubulin-binding site on the light neurofilament subunit, PLoS One 7 (2012) e49436.
[14] D. Carradori, P. Saulnier, V. Preat, A. des Rieux, J. Eyer, NFL-lipid nanocapsules for brain neural stem cell targeting in vitro and in vivo, J. Control. Release 238 (2016) 253–262.
[15] N.T. Huynh, C. Passirani, P. Saulnier, J.P. Benoit, Lipid nanocapsules: a new platform for nanomedicine, Int. J. Pharm. 379 (2009) 201–209.
[16] M.A. Curtis, R.L. Faull, P.S. Eriksson, The effect of neurodegenerative diseases on the subventricular zone, Nat. Rev. Neurosci. 8 (2007) 712.
[17] O. Gonzalez-Perez, A. Alvarez-Buylla, Oligodendrogenesis in the subventricular zone and the role of epidermal growth factor, Brain Res. Rev. 67 (2011) 147–156.
[18] T. Maki, A.C. Liang, N. Miyamoto, E.H. Lo, K. Arai, Mechanisms of oligodendrocyte regeneration from ventricular-subventricular zone-derived progenitor cells in white matter diseases, Front. Cell. Neurosci. 7 (2013) 275.
[19] H. Zhao, X. Zuo, L. Ren, Y. Li, H. Tai, J. Du, X. Xie, X. Zhang, Y. Han, Y. Wu, C. Yang, Z. Xu, H. Hong, S. Li, B. Su, Combined use of bFGF/EGF and all-trans-retinoic acid cooperatively promotes neuronal differentiation and neurite outgrowth in neural stem cells, Neurosci. Lett. 690 (2019) 61–68.
[20] B.T. Tan, L. Wang, S. Li, Z.Y. Long, Y.M. Wu, Y. Liu, Retinoic acid induced the differentiation of neural stem cells from embryonic spinal cord into functional neurons in vitro, Int. J. Clin. Exp. Pathol. 8 (2015) 8129–8135.
[21] B. Heurtault, P. Saulnier, B. Pech, J. Proust, J. Richard, J. Benoit, Lipidic Nanocapsules: Preparation Process and Use as Drug Delivery Systems, (2000) WO02688000.
[22] V.E. Miron, A. Boyd, J.W. Zhao, T.J. Yuen, J.M. Ruckh, J.L. Shadrach, P. van Wijngaarden, A.J. Wagers, A. Williams, R.J. Franklin, C. ffrench-Constant, M2 microglia and macrophages drive oligodendrocyte differentiation during CNS remyelination, Nat. Neurosci. 16 (2013) 1211–1218.
[23] D. Carradori, A.G. Dos Santos, J. Masquelier, A. Paquot, P. Saulnier, J. Eyer, V. Preat, G.G. Muccioli, M.P. Mingeot-Leclercq, A. des Rieux, The origin of neural stem cells impacts their interactions with targeted-lipid nanocapsules: potential role of plasma membrane lipid composition and fluidity, J. Control. Release 292 (2018) 248–255.
[24] K. Ito, T. Suda, Metabolic requirements for the maintenance of self-renewing stem cells, Nat. Rev. Mol. Cell Biol. 15 (2014) 243–256.
[25] J. Maia, T. Santos, S. Aday, F. Agasse, L. Cortes, J.O. Malva, L. Bernardino, L. Ferreira, Controlling the neuronal differentiation of stem cells by the intracellular delivery of retinoic acid-loaded nanoparticles, ACS Nano 5 (2011) 97–106.
[26] C. Xie, D. Cong, X. Wang, Y. Wang, H. Liang, X. Zhang, Q. Huang, The effect of simvastatin treatment on proliferation and differentiation of neural stem cells after traumatic brain injury, Brain Res. 1602 (2015) 1–8.
[27] W.F. Blakemore, R.J.M. Franklin, Remyelination in experimental models of toxin-induced demyelination, in: M. Rodriguez (Ed.), Advances in Multiple Sclerosis and Experimental Demyelinating Diseases, Springer Berlin Heidelberg, Berlin, Heidelberg, 2008, pp. 193–212.
[28] A. Lamprecht, Y. Bouligand, J.P. Benoit, New lipid nanocapsules exhibit sustained release properties for amiodarone, J. Control. Release 84 (2002) 59–68.
[29] S. Peltier, J.M. Oger, F. Lagarce, W. Couet, J.P. Benoit, Enhanced oral paclitaxel bioavailability after administration of paclitaxel-loaded lipid nanocapsules, Pharm. Res. 23 (2006) 1243–1250.
[30] P. Resnier, N. Galopin, Y. Sibiril, A. Clavreul, J. Cayon, A. Briganti, P. Legras, A. Vessieres, T. Montier, G. Jaouen, J.P. Benoit, C. Passirani, Efficient ferrocifen anticancer drug and Bcl-2 gene therapy using lipid nanocapsules on human melanoma xenograft in mouse, Pharmacol. Res. 126 (2017) 54–65.
[31] S.J. Lim, C.K. Kim, Formulation parameters determining the physicochemical characteristics of solid lipid nanoparticles loaded with all-trans retinoic acid, Int. J. Pharm.Stem Cells Transl. Med. 243 (2002) 135–146.
[32] G.A. Castro, R.L. Orefice, J.M. Vilela, M.S. Andrade, L.A. Ferreira, Development of a new solid lipid nanoparticle formulation containing retinoic acid for topical treatment of acne, J. Microencapsul. 24 (2007) 395–407.
[33] R.J. Li, X. Ying, Y. Zhang, R.J. Ju, X.X. Wang, H.J. Yao, Y. Men, W. Tian, Y. Yu, L. Zhang, R.J. Huang, W.L. Lu, All-trans retinoic acid stealth liposomes prevent the relapse of breast cancer arising from the cancer stem cells, J. Control. Release 149 (2011) 281–291.
[34] C. Lepinoux-Chambaud, K. Barreau, J. Eyer, The neurofilament-derived peptide NFL-TBS.40-63 targets neural stem cells and affects their properties, Stem Cells Transl.Med. 5 (2016) 901–913.
[35] E. Pastrana, V. Silva-Vargas, F. Doetsch, Eyes wide open: a critical review of sphere-formation as an assay for stem cells, Cell Stem Cell 8 (2011) 486–498.
[36] C.B. Johansson, S. Momma, D.L. Clarke, M. Risling, U. Lendahl, J. Frisen, Identification of a neural stem cell in the adult mammalian central nervous system, Cell 96 (1999) 25–34.
[37] M.T. De Angelis, E.I. Parrotta, G. Santamaria, G. Cuda, Short-term retinoic acid treatment sustains pluripotency and suppresses differentiation of human induced pluripotent stem cells, Cell Death Dis. 9 (2018) 6.
[38] R. Wang, J. Liang, H.M. Yu, H. Liang, Y.J. Shi, H.T. Yang, Retinoic acid maintains self-renewal of murine embryonic stem cells via a feedback mechanism, Differ.; Res. Biol. Divers. 76 (2008) 931–945.
[39] T.H. Hsieh, C.Y. Hsu, C.F. Tsai, C.C. Chiu, S.S. Liang, T.N. Wang, P.L. Kuo, C.Y. Long, E.M. Tsai, A novel cell-penetrating peptide suppresses breast tumorigenesis by inhibiting beta-catenin/LEF-1 signaling, Sci. Rep. 6 (2016) 19156.
[40] N.A. Capurso, M. Look, L. Jeanbart, H. Nowyhed, C. Abraham, J. Craft, T.M. Fahmy, Development of a nanoparticulate formulation of retinoic acid that suppresses Th17 cells and upregulates regulatory T cells, Self Nonself 1 (2010) 335–340.
[41] J. Bianco, D. Carradori, R. Deumens, A. des Rieux, Rapid serum-free isolation of oligodendrocyte progenitor cells from adult rat spinal cord, Stem Cell Rev Rep 13 (2017) 499–512.
[42] M. Hattori, K. Shimizu, K. Katsumura, H. Oku, Y. Sano, K. Matsumoto, Y. Yamaguchi, T. Ikeda, Effects of all-trans retinoic acid nanoparticles on corneal epithelial wound healing, Graefes Arch. Clin. Exp. Ophthalmol. 250 (2012) 557–563.
[43] R. Käkelä, S. Laitinen, L. Kilpinen, P. Lehenkari, Lipids modulate stem/progenitor cell function, in: V.B. Patel (Ed.), The Molecular Nutrition of Fats, Academic Press, 2019, pp. 403–417.
[44] M.E. Pak, D.H. Jung, H.J. Lee, M.J. Shin, S.Y. Kim, Y.B. Shin, Y.J. Yun, H.K. Shin, B.T. Choi, Combined therapy involving electroacupuncture and treadmill exercise attenuates demyelination in the corpus callosum by stimulating oligodendrogenesis in a rat model of neonatal hypoxia-ischemia, Exp. Neurol. 300 (2018) 222–231.
[45] C.L. Cullen, M. Senesi, A.D. Tang, M.T. Clutterbuck, L. Auderset, M.E. O'Rourke, J. Rodger, K.M. Young, Low-intensity transcranial magnetic stimulation promotes the survival and maturation of newborn oligodendrocytes in the adult mouse brain, Glia 67 (2019) 1462–1477.
[46] T.A. Olmstead, P.A. Chiarelli, D.J. Griggs, A.M. McClintic, A.N. Myroniv, P.D. Mourad, Transcranial and pulsed focused ultrasound that activates brain can accelerate remyelination in a mouse model of multiple sclerosis, J. Ther. Ultrasound 6 (2018) 11.
[47] X. Li, S.Y. Tzeng, C.G. Zamboni, V.E. Koliatsos, G.L. Ming, J.J. Green, H.Q. Mao, Enhancing oligodendrocyte differentiation by transient transcription activation via DNA nanoparticle-mediated transfection, Acta Biomater. 54 (2017) 249–258.
[48] S.C. Starossom, J. Campo Garcia, T. Woelfle, S. Romero-Suarez, M. Olah, F. Watanabe, L. Cao, A. Yeste, J.J. Tukker, F.J. Quintana, J. Imitola, F. Witzel, D. Schmitz, M. Morkel, F. Paul, C. Infante-Duarte, S.J. Khoury, Chi3l3 induces oligodendrogenesis in an experimental model of autoimmune neuroinflammation, Nat. Commun. 10 (2019) 217.
[49] S. Rittchen, A. Boyd, A. Burns, J. Park, T.M. Fahmy, S. Metcalfe, A. Williams, Myelin repair in vivo is increased by targeting oligodendrocyte precursor cells with nanoparticles encapsulating leukaemia inhibitory factor (LIF), Biomaterials 56 (2015) 78–85.
[50] Q. Zhang, W. Zhu, F. Xu, X. Dai, L. Shi, W. Cai, H. Mu, T.K. Hitchens, L.M. Foley, X. Liu, F. Yu, J. Chen, Y. Shi, R.K. Leak, Y. Gao, J. Chen, X. Hu, The interleukin-4/PPARgamma signaling axis promotes oligodendrocyte differentiation and remyelination after brain injury, PLoS Biol. 17 (2019) e3000330.
[51] R.H. Woodruff, R.J. Franklin, Demyelination and remyelination of the caudal cerebellar peduncle of adult rats following stereotaxic injections of lysolecithin, ethidium bromide, and complement/anti-galactocerebroside: a comparative study, Glia 25 (1999) 216–228.
[52] D. de Paula Faria, E.F. de Vries, J.W. Sijbesma, C.A. Buchpiguel, R.A. Dierckx, S.C. Copray, PET imaging of glucose metabolism, neuroinflammation and demyelination in the lysolecithin rat model for multiple sclerosis, Mult. Scler. 20 (2014) 1443–1452.
[53] A.J. Roskams, X. Cai, G.V. Ronnett, Expression of neuron-specific beta-III tubulin during olfactory neurogenesis in the embryonic and adult rat, Neuroscience 83 (1998) 191–200.
[54] R. Krencik, J.P. Weick, Y. Liu, Z.J. Zhang, S.C. Zhang, Specification of transplantable astroglial subtypes from human pluripotent stem cells, Nat. Biotechnol. 29 (2011) 528–534.
[55] M.J. Godinho, L. Teh, M.A. Pollett, D. Goodman, S.I. Hodgetts, I. Sweetman, M. Walters, J. Verhaagen, G.W. Plant, A.R. Harvey, Immunohistochemical, ultrastructural and functional analysis of axonal regeneration through peripheral nerve grafts containing Schwann cells expressing BDNF, CNTF or NT3, PLoS One 8 (2013) e69987.
[56] W. Liedtke, W. Edelmann, P.L. Bieri, F.C. Chiu, N.J. Cowan, R. Kucherlapati, C.S. Raine, GFAP is necessary for the integrity of CNS white matter architecture and long-term maintenance of myelination, Neuron 17 (1996) 607–615.
[57] H.E. Marei, Z. Shouman, A. Althani, N. Afifi, AEA, S. Lashen, A. Hasan, T. Caceci, R. Rizzi, C. Cenciarelli, P. Casalbore, Differentiation of human olfactory bulb-derived neural stem cells toward oligodendrocyte, J. Cell. Physiol. 233 (2018) 1321–1329.
[58] T. Lin, Z. Xiang, L. Cui, W. Stallcup, S.A. Reeves, New mouse oligodendrocyte precursor (mOP) cells for studies on oligodendrocyte maturation and function, J. Neurosci. Methods 157 (2006) 187–194.
[59] X. Zhu, D.E. Bergles, A. Nishiyama, NG2 cells generate both oligodendrocytes and gray matter astrocytes, Development 135 (2008) 145–157.
[60] S.A. Goldman, N.J. Kuypers, How to Make an Oligodendrocyte, 142 Development, 2015, pp. 3983–3995.
[61] A.F. Lloyd, C.L. Davies, R.K. Holloway, Y. Labrak, G. Ireland, D. Carradori, A. Dillenburg, E. Borger, D. Soong, J.C. Richardson, T. Kuhlmann, A. Williams, J.W. Pollard, A. des Rieux, J. Priller, V.E. Miron, Central nervous system regeneration is driven by microglia necroptosis and repopulation, Nat. Neurosci. 22 (2019) 1046–1052.
[62] M. Machado-Pereira, T. Santos, L. Ferreira, L. Bernardino, R. Ferreira, Anti-Inflammatory Strategy for M2 Microglial Polarization Using Retinoic Acid-Loaded Nanoparticles, Mediators Inflamm, 2017, p. 6742427 (2017).
[63] S. Kanakasabai, E. Pestereva, W. Chearwae, S.K. Gupta, S. Ansari, J.J. Bright, PPARgamma agonists promote oligodendrocyte differentiation of neural stem cells by modulating stemness and differentiation genes, PLoS One 7 (2012) e50500.
[64] K. Azim, O. Raineteau, A.M. Butt, Intraventricular injection of FGF-2 promotes generation of oligodendrocyte-lineage cells in the postnatal and adult forebrain, Glia 60 (2012) 1977–1990.
[65] T. Santos, R. Ferreira, J. Maia, F. Agasse, S. Xapelli, L. Cortes, J. Braganca, J.O. Malva, L. Ferreira, L. Bernardino, Polymeric nanoparticles to control the differentiation of neural stem cells in the subventricular zone of the brain, ACS Nano 6 (2012) 10463–10474.